J Plant Physiol. Author manuscript; available in PMC 2016 May 12.

Published in final edited form as:
J Plant Physiol. 2016 May 1; 194: 2–12. doi:10.1016/j.jplph.2015.09.002.

Living in biological soil crust communities of African deserts—Physiological traits of green algal *Klebsormidium* species (Streptophyta) to cope with desiccation, light and temperature gradients

Ulf Karsten[a,*], **Klaus Herburger**[b], and **Andreas Holzinger**[b]

[a]University of Rostock, Institute of Biological Sciences, Applied Ecology & Phycology, Albert-Einstein-Strasse 3, D-18059 Rostock, Germany

[b]University of Innsbruck, Institute of Botany, Functional Plant Biology, Sternwartestrasse 15, A-6020 Innsbruck, Austria

Abstract

Green algae of the genus *Klebsormidium* (Klebsormidiales, Streptophyta) are typical members of biological soil crusts (BSCs) worldwide. The phylogeny and ecophysiology of *Klebsormidium* has been intensively studied in recent years, and a new lineage called superclade G, which was isolated from BSCs in arid southern Africa and comprising undescribed species, was reported. Three different African strains, that have previously been isolated from hot-desert BSCs and molecular-taxonomically characterized, were comparatively investigated. In addition, *Klebsormidium subtilissimum* from a cold-desert habitat (Alaska, USA, superclade E) was included in the study as well. Photosynthetic performance was measured under different controlled abiotic conditions, including dehydration and rehydration, as well as under a light and temperature gradient.

All *Klebsormidium* strains exhibited optimum photosynthetic oxygen production at low photon fluence rates, but with no indication of photoinhibition under high light conditions pointing to flexible acclimation mechanisms of the photosynthetic apparatus. Respiration under lower temperatures was generally much less effective than photosynthesis, while the opposite was true for higher temperatures. The *Klebsormidium* strains tested showed a decrease and inhibition of the effective quantum yield during desiccation, however with different kinetics. While the single celled and small filamentous strains exhibited relatively fast inhibition, the uniserate filament forming isolates desiccated slower. Except one, all other strains fully recovered effective quantum yield after rehydration. The presented data provide an explanation for the regular occurrence of *Klebsormidium* strains or species in hot and cold deserts, which are characterized by low water availability and other stressful conditions.

*Corresponding author. ulf.karsten@uni-rostock.de (U. Karsten) .

Europe PMC Funders Author Manuscripts

Keywords

Aeroterrestrial algae; Biological soil crust; Ecophysiology; Morphology; Photosynthesis; Respiration

1. Introduction

On a global scale, biological soil crust communities (BSCs) form the most productive microbial biomass of the Earth's 'Critical Zone'. This zone is also defined as heterogeneous, near surface environment in which complex interactions involving rock surfaces, soil, water, air and living organisms regulate the natural habitat, and hence determine the availability of life-sustaining resources (Belnap and Lange, 2001). In newly created non-vegetated or disturbed landscapes, such as volcanic areas, glacier forefields, flood plains and many drylands, BSCs represent the pioneer communities that form the basis for further ecosystem development (Yoshitake et al., 2010). BSCs consist of living organisms such as algae, cyanobacteria and lichens, and are characterized as 'ecosystem-engineers' forming water-stable aggregates that have multi-functional ecological roles in primary production, nutrient and hydrological cycles, mineralization, dust trapping, weathering and stabilization of soils (e.g. Castillo-Monroy et al., 2010). Due to the extracellular matrix of cyanobacteria and algae, soil particles are aggregated forming a carpet-like biofilm, which reduces erosion by wind and water. A recent review clearly indicated the important ecological role of BSCs for global carbon (C) fixation (about 7% of terrestrial vegetation) and N fixation (about 50% of terrestrial biological N fixation) (Elbert et al., 2012).

Terrestrial filamentous green algae of the cosmopolitan genus *Klebsormidium* (Klebsormidiophyceae, Streptophyta) are often abundant components of terrestrial and freshwater habitats, such as rivers, lakes, bogs, soil, rock surfaces, tree bark, sand dunes, and BSCs from alpine regions or even deserts (Rindi et al., 2011; Karsten and Holzinger, 2014; and references therein). Rindi et al. (2011) provided so far the most comprehensive phylogeny of this genus using ITS rRNA and rbcL sequences. These authors showed seven main superclades A–G; which included sixteen well-supported clades. While superclade A contained species of the closely related genus *Interfilum* (Mikhailyuk et al., 2008; Rindi et al., 2011), superclades B–F comprised all *Klebsormidium* species so far described. Most interesting, a new lineage of *Klebsormidium* termed superclade G, which was isolated from BSCs in arid southern Africa and comprising undescribed species, was for the first time reported (Rindi et al., 2011). Mikhailyuk et al. (2014) demonstrated that the known *Klebsormidium* species differed in their ultrastructure and texture of cell walls. Members of the superclades B, C and E were characterized as mesophytic and hydrophytic lineages, because they exhibited filaments with gelatinized cell walls that easily transform into short filaments or even into individual cells (Mikhailyuk et al., 2014). In contrast, specimens of the superclades D, F and G were suggested as xerophytic lineages because of dense and rather strong filaments without mucilage (Mikhailyuk et al., 2014). These authors described superclade G members also as typical African group. This was again supported by Ryšánek et al. (2015) who mentioned that although collecting 200 *Klebsormidium* strains from Europe, North America and Asia, they could not find a single genotype of superclade G.

Because of the wide biogeographic distribution and occurrence in so diverse environments, the physiological traits of various *Interfilum* and *Klebsormidium* species have been recently studied concerning acclimation mechanisms against desiccation, temperature, visible light; UVR and pH gradients (Karsten et al., 2010, 2014; Holzinger and Karsten, 2013; Holzinger et al., 2011, 2014; Kaplan et al., 2012; Kitzing et al., 2014; Škaloud et al., 2014; Kitzing and Karsten, 2015). The emerging picture is that most of the species investigated so far were members of the superclades A–F, and that depending on the superclade membership the physiological response patterns such as desiccation tolerance can be quite different as exemplarily described for the two coexisting *Klebsormidium dissectum* (superclade E) and *Klebsormidium crenulatum* (superclade F) in alpine BSC communities of the Alps (Karsten et al., 2010; Karsten and Holzinger, 2012). The variability in the desiccation tolerance of both *Klebsormidium* species can be explained by differences in their morphological and structural features such as strong versus weak filaments (Karsten et al., 2010; Holzinger et al., 2011; Karsten and Holzinger, 2012). Moreover these differences may be attributed to different physiological traits, e.g. *K. crenulatum* (superclade F) has been shown to have a more negative water potential ($\Psi = -2.09$ MPa) compared to *K. nitens* (superclade E, $\Psi = -1.67$ MPa) (Kaplan et al., 2012).

Ullmann and Büdel (2001) were the first who provided an overview on the distribution of BSCs over Africa, pointing to a concentration of these microbiotic communities in the southern and southwestern part of the continent. Later and in a more comprehensive way, Büdel et al. (2009) undertook an intensive field monitoring and sampling in drylands along a transect stretching from the Namibian–Angolan border down south to the Cape Peninsula. These authors reported seven BSC types which could be differentiated on the basis of morphology and taxonomic composition, and documented 29 green algal species including some undescribed *Klebsormidium* species. Büdel et al. (2009) concluded that BSCs are a normal and frequent vegetation element in arid and semi-arid southwestern Africa, and that rain frequency and duration of dry periods rather than total annual precipitation are the ecological key factors for the development, differentiation and composition of the microbiotic communities.

As ecophysiological studies on green algae from African hot desert BSCs are missing, and because of this conspicuously different superclade G in the *Klebsormidium* phylogeny, our major goal was to characterize for the first time some of the available strains. Photosynthetic activity under controlled dehydration and recovery conditions and along temperature and light gradients were comparatively investigated in three African *Klebsormidium* strains. For comparison, *Klebsormidium subtilissimum* from a cold-desert habitat (Alaska, USA, superclade E) was included in the study as well. The main hypothesis was to evaluate whether physiological traits are present which influence desiccation, temperature and light tolerance in these specific *Klebsormidium* genotypes. Of particular interest was to consider whether the environmental conditions of the original habitat are reflected in the respective response patterns.

2. Materials and methods

2.1. Strain origin and culture conditions

The Klebsormidium strains of the superclade G - BIOTA 14.614.7 (= African Strain A), BIOTA 14.613.5e (= African Strain B) and BIOTA 14.614.18.24 (= African Strain C)—were originally collected and isolated by Prof. Burkhard Büdel in the frame of the international BIOTA project (Büdel et al., 2009), and kindly provided for the present study. The species *Klebsormidium subtilissimum* SAG 384-1 (= Arctic Strain) was purchased from The Culture Collection of Algae at Göttingen University; Germany (international acronym SAG; http://www.uni-goettingen.de/en/184982.html). Detailed data on habitat and origin, meteorological data, as well as taxonomic assignments are summarized in Table 1.

The 4 *Klebsormidium* stock cultures were maintained in Erlenmeyer flasks (volume 250–500 mL) filled with modified Bold's Basal Medium (3NBBM; Starr and Zeikus, 1993), which is a highly enriched purely inorganic medium containing various trace metals, few vitamins and triple nitrate concentration, but no carbon source. Identical culture conditions and equipment was applied as described for *Klebsormidium dissectum* (Karsten and Holzinger, 2012), i.e. cells were kept at 20 °C and 35–40 μmol photons m^{-2} s^{-1} under a light-dark cycle of 16:8 h L:D (Osram Daylight Lumilux Cool White lamps L36W/840, Osram, Munich, Germany). Photon fluence rate measurements were untertaken with a Solar Light PMA 2132 cosine corrected PAR sensor connected to a Solar Light PMA 2100 radiometer (Solar Light Co. Inc., Philadelphia, USA). For all experiments always vital log-phase cultures exhibiting comparable cell densities were used.

2.2. Light microscopy

Algae of log-phase cultures used for physiological measurements (African Strains A–C, Arctic Strain) were also investigated with a Zeiss Axiovert 200 M microscope (Carl Zeiss Microscopy GmbH, Jena, Germany), equipped with a 100 × 1.3 NA objective lens and an Axiocam MRc5 camera controlled by Zeiss Axiovision software. For contrast enhancement, differential interference contrast (DIC) was applied. Further processing of images was performed using Adobe Photoshop (CS5) software version 12.1 (Adobe Systems, San Jose, CA, USA). Cell dimensions (cell width and length) were determined by measuring a minimum of 20 cells and the length:width (L:W) ratio was calculated. Mean values ± SD are shown.

2.3. Dehydration and recovery experiments

For the desiccation experiments a new highly standardized setup was applied to follow the kinetics of controlled dehydration and subsequent rehydration on the effective quantum yield of photosystem II (PSII) using non-invasive pulse amplitude modulation (PAM) fluorometry (Karsten et al., 2014). Always low-light acclimated samples (35–40 μmol photons m^{-2} s^{-1}) were measured with a PAM 2500 (Heinz Walz GmbH, Effeltrich, Germany). Cells of each *Klebsormidium* isolate were concentrated as small light green spots on 4 replicate Whatman GF/F glass fibre filters (Whatman, Dassel, Germany). Onto each filter exactly 200 μL of the respective homogeneous algal suspension (c. 1–2 mg chlorophyll a L^{-1}) was applied using an Eppendorf pipette. Using defined starting volumes of log-phase cultures guaranteed

reproducibility, since it is difficult or impossible to obtain reliable water contents in small quantities of algal filaments. The moist filters were positioned on perforated metal grids on top of four glass columns inside a transparent 200 mL polystyrol box. Each of these boxes was filled with 100 g of freshly activated silica gel (Silica Gel Orange, Carl Roth, Karlsruhe, Germany) and sealed with a transparent top lid. The relative air humidity (RH) conditions inside the boxes were recorded with a PCE-MSR145S-TH mini data logger for air humidity and temperature (PCE Instruments, Meschede, Germany). The data showed that within the first 30 min the RH declines from about 30% to 10% and remains after that almost unchanged at this low air humidity pointing to a reproducible dry atmosphere (Karsten et al., 2014). The chambers were maintained at 22 ± 1 °C and 40 μmol photons m^{-2} s^{-1} PAR (culture conditions) (Osram light sources see above) which reflects the natural average temperatures in the habitats of the dessert strains and prevents light stress during measurements (Karsten et al., 2014).

The effective quantum yield (ΔF/Fm') of photosystem II (PSII) was regularly determined during the dehydration period (up to 500 min depending on the strain) using the PAM 2500 according the approach of Genty et al. (1989). ΔF/Fm′ was calculated as $(F_m'–F)/F_m'$ with F as the fluorescence yield of light-treated algal cells (40 μmol photons m^{-2} s^{-1}) and F_m' as the maximum light-adapted fluorescence yield after employing a 800 ms saturation pulse as described by Schreiber and Bilger (1993). The PAM light probe was positioned outside the cover lid of the boxes (always 2 mm distance) to guarantee undisturbed RH conditions inside, i.e. all fluorescence measurements were performed through the polystyrol lids. The distance from the PAM light probe to the algal sample onto the glass fibre filters was always kept constant at 10 mm. Since the water content of the applied small cell numbers (200 μL suspension) is almost impossible to estimate, we undertook preliminary experiments using 25–50 times higher quantities of algal biomass, and estimated that the final remaining water content after controlled desiccation using the described approach was between 5 and 10% of the control (data not shown). While our desiccation set-up guarantees comparative and reproducible starting and end points of cellular water contents, it fails to describe any kinetics of water loss.

After the dehydration period, the dried glass fibre filters were transferred to a new polystyrol box which was filled with 100 mL tap water instead of silica gel to create a high humidity atmosphere (>95%). The filters were rehydrated by adding 200 μL of the standard growth medium to each algal spot and recovery of $(F_m'–F)/F_m'$ was followed with the same methodology as described above.

2.4. Photosynthesis and respiration under light and temperature gradients

A Presens Fibox 3 oxygen optode (Presens, Regensburg, Germany) was applied to record photosynthetic oxygen production rates under rising photon fluence densities (PI curves) and respiratory oxygen consumption in the dark. The oxygen sensor was attached to a 3 mL thermostatic acrylic chamber (type DW1, Hansatech Instruments, Norfolk, UK) combined with a magnetic stirrer according to Remias et al. (2010) to ensure homogenous light absorption. Always 2.8 mL log-phase *Klebsormidium* suspensions of known chlorophyll *a* concentration were added to the chamber supplemented by 0.2 mL of a $NaHCO_3$ stock

solution (resulting in 2 mM $NaHCO_3$ final concentration) to guarantee sufficient carbon supply during measurements. The light path inside the measuring chamber was 10 mm, and the applied light levels were carefully determined with a Hansatech QRT1 PAR sensor (Hansatech Instruments, Norfolk, UK). This quantum sensor was vertically positioned inside the cuvette allowing light source (halogen lamp) calibration from the side (90° angle) and thereby overcoming the potential difficulties associated with accurately measuring PAR light levels within the small chamber. Before the onset of increasing photon fluence rates respiration was measured in darkness followed by exposure of the algal cells to nine light levels ranging from 0 to 500 µmol photons m^{-2} s^{-1} PAR (photosynthetically active radiation for 10 min) at 22 °C using a combination of 4 different Hansatech A5 neutral filters (Hansatech Instruments, Norfolk, UK). All O_2 rates were normalised to total chlorophyll *a* concentration, ranging from 3 to 6 µg 3 mL $^{-1}$, which were determined after each PI curve measurement. We used chlorophyll *a* concentration as reference parameter, because cell densities of the 4 *Klebsormidium* strains were difficult to determine because of the filamentous morphology and the fact of uncontrolled disintegration into smaller fragments of some of the isolates. The 3 mL *Klebsormidium* suspension was filtered onto a Whatman GF/F glass fibre filter using a glass Pasteur pipette, and chlorophyll *a* and *b* extracted by adding 3 mL dimethyl formamide (DMF) followed by photometric quantification (Porra et al., 1989). PI curve data of the 3 African Strains were calculated and fitted with the mathematical photosynthesis model of Webb et al. (1974), which allowed the calculation of the four characteristic parameters: α, positive slope at limiting photon fluence rates (µmol O_2 h^{-1} mg^{-1} Chl. *a* (µmol photons m^{-2} s^{-1})$^{-1}$; I_c, light compensation point (µmol photons m^{-2} s^{-1}); I_k, initial value of light-saturated photosynthesis (µmol photons m^{-2} s^{-1}). Furthermore, the maximum photosynthetic rate in the light-saturated range (µmol O_2 h^{-1} mg^{-1} Chl. *a*) was calculated.

Since with the halogen lamp of the oxygen optode system only 500 µmol photons m^{-2} s^{-1} could be realized (see above), a PAM 2500 was additionally used to apply photon fluence rates up to 1432 µmol photons m^{-2} s^{-1} for the determination of light-induced rETR and possible photoinhibitory effects. Cells of each *Klebsormidium* strain were transferred on 4 replicate Whatman GF/F glass fibre filters until a light green spot was visible. These moist filters were also positioned in the transparent 200 mL, tap water filled polystyrol boxes, and treated as already described. Algal cells were exposed to 13 photon fluence densities (PFDs) for 30 s each (rapid light curves) ranging from 1 up to 1432 µmol photons m^{-2} s^{-1}. The actinic light was provided by a red power LED (630 nm) of the PAM 2500. After each light exposure, a saturating pulse was given to detect F_m and $\Delta F/F_m'$. The relative electron transport rate of PSII (rETR) was calculated according to Kromkamp and Forster (2003):

$$\mathrm{rETR} = \Delta F / F_m' \mathrm{PFD} \quad (1)$$

where $\Delta F/F_m'$ = the effective PSII quantum efficiency and PFD = photon flux density.

All measurements were undertaken under at 22 ± 1 °C. Photosynthesis-irradiance (PI) curves as rETR vs. PFD were calculated to check whether the 4 strains of *Klebsormidium* exhibit indications of photoinhibition.

The effect of rising temperatures on photosynthetic and respiratory response patterns (referenced to chlorophyll *a*) in the four *Klebsormidium* strains was determined using a Thermo Haake K20 refrigerated circulator (Thermo Fisher Scientific Inc., Waltham, Massachusetts, USA) connected to the measuring chamber. All algal isolates were exposed to nine temperature steps ranging from 5 to 45 °C in 5 °C increments according to Karsten and Holzinger (2012). After treatment with the highest temperature (45 °C) photosynthesis and respiration were measured again after a temperature reduction to 30 °C to look for recovery effects.

From the final photosynthetic and respiratory rates (μmol O_2 mg^{-1} Chl. a h^{-1}) the gross photosynthesis:respiration (P:R) ratios for each temperature were calculated.

2.5. Statistical analysis

All oxygen measurements (optode) were carried out with three independent replicates (n = 3) while all measurement of the effective quantum yield (performed by PAM) were performed in four independent replicates (n = 4). The shown data represent the respective mean values ± standard deviation.

Statistical significance of the means of the effective quantum yield of dehydrated and rehydrated samples, as well as all optode data were tested with one-way ANOVA followed by a Tukey's multiple comparison test to find subgroups of means with significant differences. Analyses were performed with InStat (GraphPad Software Inc., La Jolla, CA, USA).

3. Results

3.1. Light microscopy

The African Strain A formed uniserate filaments and each cell contained one parietal chloroplast with a prominent pyrenoid surrounded by starch grains (Fig. 1a). The chloroplast covered the whole length of the cell and about 2/3 of the cell circumference, while the central part of one longitudinal margin often protruded distinctly towards the cell centre (Fig. 1a). Most cross cell walls exhibited protuberances of wall material on one or opposite sides of the same cross cell wall and occasionally the cross wall appeared swollen (Fig. 1a). Fragmentation into small cell filaments (2–6 cells) was scarcely. The cell diameter was homogenously (Table 2), while the cell length varied more (Table 2), resulting in a cell lengh:width (L:W) ratio of 1.2 ± 0.2 (Table 2). Cells of African Strain B were significantly (P < 0.001) narrower, but the cell length did not differ significantly (P < 0.001) from African Strain A (Table 2). African Strain B occurred unicellularly and the parietal chloroplast was less expanded, covering 1/3–2/3 of the cell and usually did not reach towards the poles of the ovoid or cylindrical cells (Fig. 1b). The longitudinal margins of the chloroplast were smooth and it exhibited one poorly developed pyrenoid (Fig. 1b). Cells were surrounded by a thin mucilage layer (Fig. 1b). The cell shape of the Arctic Strain appeared similar to African Strain B, however, they were significantly wider and longer (Fig. 1c, Tab. 2). Filaments showed a strong tendency to disintegration and most filaments contained 2–4 cells. Each cell exhibited one parietal chloroplast embedding a small pyrenoid (Fig. 1c). The longitutinal

margins of the chloroplast were smooth (Fig. 1c). Some cross cell walls exhibited protuberances of wall material on opposite sides of the same cross wall (Fig. 1c). Cells were significantly longer compared to the other three strains, resulting in a L:R ratio of 2.5 ± 0.8 (Tab. 2). African Strain C formed uniserate filaments and the cell width and length did not differ significantly from each other ($P < 0.001$; Table 2, Fig. 1d). Each cell contained one chloroplast touching the cross walls and covering ~3/4 of the cell circumference (Fig. 1d). The longitudinal margins of the chloroplast were smooth and it contained one clearly visible pyrenoid surrounded by starch grains (Fig. 1d). Sometimes, prominent cross wall protuberances occurred (Fig. 1d).

3.2. Light requirements of photosynthesis

The photosynthetic oxygen production was stimulated by rising photon fluence densities in all 4 *Klebsormidium* isolates as reflected in PI curves from which characteristic parameters for the description of the light requirements were derived (Fig. 2; Table. 3). African Strains B and C and the Arctic Strain exhibited light-saturated PI curves with maximum oxygen production rates between 137.5 and 182.9 μmol O_2 h^{-1} mg^{-1} Chl. a. In contrast, African Strain A did not reach light-saturation up to the applied 500 μmol photons m^{-2} s^{-1}, resulting in a maximum oxygen production of only 79 μmol O_2 h^{-1} mg^{-1} Chl. *a* (Fig. 2). None of the investigated *Klebsormidium* samples exhibited any indication of photoinhibition, at least up to the highest photon fluence rate of 500 μmol photons m^{-2} s^{-1} tested. To double check that indeed no photoinhibition is visible in the 4 *Klebsormidium* strains, relative electron transport rates as function of increasing photon fluence rate up to 1432 μmol photons m^{-2} s^{-1} were measured (Fig. 3), and no photoinhibitory effect could be determined. While African Strain A showed a relatively low α value (photosynthetic efficiency in the light limited range) of 5.73 μmol O_2 h^{-1} mg^{-1} Chl. *a* (μmol photons m^{-2} s^{-1})$^{-1}$, this value was significantly higher in the African Strains B and C and the Arctic Strain ($p < 0.05$) (Table 3). The 4 *Klebsormidium* strains exhibited rather similar I_c values (light compensation point) between 4.4 and 14.7 μmol photons m^{-2} s^{-1}, and I_k values (initial light saturation point) ranging from 14.1 to 23.6 μmol photons m^{-2} s^{-1} (Table 3), all of which clearly point to low light requirements for photosynthesis (Fig. 2). In addition, the Chl. *a* to Chl. *b* ratios in all investigated strains were similar between 1.86 and 2.43 (Table 3)

3.3. Temperature requirements of photosynthesis and respiration

The effect of increasing temperatures on gross photosynthetic oxygen production and respiratory oxygen consumption in the 4 *Klebsormidium* strains clearly pointed to isolate-specific differences (Fig. 4). The African Strains A and C showed a similar response pattern with rising photosynthetic activity from low values at 5–10 °C up to maximum values between 30 and 35 °C, followed by a sharp decline and complete inhibition between 35 and 45 °C (Fig. 4). Although African Strain B exhibited also low oxygen evolution rates between 5 and 10 °C, and optimum photosynthesis at 30–35 °C, this strain could much better cope with 40 °C where still 50% of the maximum could be recorded, while at 45 °C photosynthesis was not detectable (Fig. 4). In contrast, the Arctic Strain showed already at 5 and 10 °C relatively high oxygen evolution rates, and a broad optimum photosynthetic activity between 15 and 35 °C, followed by a drastic loss at 40 and 45 °C (Fig. 4).

In all samples respiration at 5 and 10 °C was not detectable or very low, while temperatures between >10 °C and 30–35 °C led to a continuous, and almost linear increase in respiratory activity up to the maximum values between −41.4 and −84.9 μmol O_2 h^{-1} mg^{-1} Chl. a ($p < 0.001$) (Fig. 4). Further increases in temperature up to 45 °C led to a moderate decrease in respiration of African Strain C, while the remaining *Klebsormidium* strains showed an unaffected respiratory rate at this high temperature (Fig. 4). The photosynthesis and respiration data indicate conspicuously different temperature requirements for both physiological processes.

After treating all samples with 45 °C, temperature was decreased to 30 °C and the short-term recovery potential of photosynthesis and respiration evaluated (Fig. 5). The three African Strains showed very similar response patterns, i.e. with declining temperatures the negative photosynthethic rates partially recovered to zero or slightly positive values. But also the respiratory activity returned to low rates. In contrast, the Arctic Strain exhibited less high, but still strong negative photosynthetic activity and a respiration value similar to that between 20 and 25 °C (Fig. 5).

The photosynthesis:respiration quotient (P:R) in all 4 *Klebsormidium* isolates decreased with increasing temperatures ($p < 0.001$) (Fig. 6). While at 5 °C the highest P:R value was only observed in African Strain A, all other samples showed an increase from 5 to 10 °C (maximum value) followed by a continuous decrease (Fig. 6). The P:R ratios dropped in all investigated *Klebsormidium* isolates to negative values, i.e. in African Strains B and C only at 45 °C, in African Strain A at 40 and 45 °C, and in the Arctic Strain already at 30 °C and all higher temperatures (Fig. 6).

3.4. Dehydration and rehydration

The standardized methodological approach with the silica gel filled polystyrol boxes and PAM measurements from the outside allowed comparative effective quantum yield determinations in all *Klebsormidium* samples during the dehydration and rehydration intervals, indicating different response patterns (Figs. 7, 8). While African Strain B showed a continuous decrease of ΔF/Fm′ from beginning on over a period of 350 min down to zero signal, all other isolates exhibited an unchanged maximum effective quantum yield for some time before a threshold was reached after which the fluorescence signals strongly dropped to values between 0 and 20% (Fig. 7). The interval of unaffected ΔF/Fm′ was 230–250 min in the African Strains A and C and, and only 100 min in the Arctic Strain. After these periods the effective quantum yield decreased within 100 to 130 min to zero in both African Strains, while it took >200 min to reach 20% of the control in the Arctic Strain, which was the minimum signal (Fig. 7).

After 500 min dehydration interval all *Klebsormidium* samples were rehydrated. While both African Strains B and C together with the Arctic Strain fully recovered within 1000–1500 min, in African Strain A only 20% of the control ΔF/Fm′ values were recorded, even after a 2000 min rehydration interval (Fig. 8). African Strain C exhibited the fasted recovery kinetics.

4. Discussion

4.1. Habitat and phylogeny

In the present study, we examined for the first time the morphology and ecophysiological traits of three different strains of *Klebsormidium* isolated from BSC communities of the succulent Karoo, South Africa which is known as semi-arid hot desert (Büdel et al., 2009). This region is characterized by high temperatures and extremely low precipitation ranging from 0 to 34.2 mm per month resulting in an annual rainfall of only 56 mm (Table 1). The investigated BIOTA strains belong phylogenetically to the *Klebsormidium* superclade G (Rindi et al., 2011), which is described only as so-called 'African clade' without any further information on taxonomy or physiology. For comparison we selected *Klebsormidium subtilissimum* from a cold-desert habitat (Alaska, USA, superclade E), which is characterized by much lower temperatures, but also relatively low precipitation ranging from 2.3 to 26.7 mm per month summing up to an annual rain-/snowfall of 114 mm (Table 1). In contrast to the three African strains, *K. subtilissimum* (Arctic Strain) is a well described species (Fig. 1C) (Silva et al., 1972). The three African Strains A, B and C exhibited significantly different morphologies particularly reflected in the cell width which ranged from 4.1 to 8.8 μm (Fig. 1A, B and D, Table. 2). They all were grown for long time under identical controlled conditions and hence any potential environmental effect on the morphology can be excluded. Consequently, we assume that the three African *Klebsormidium* strains represent new species, which have still to be described.

4.2. Light requirements of photosynthesis

The PI-curve parameters α, I_c and I_k only revealed small differences among the investigated four *Klebsormidium* isolates (Fig. 2, Table. 3), while the all α values can be considered as high and those of I_c and I_k as very low. The investigated samples thus all exhibit very minor light requirements for saturated photosynthesis, which has been reported before for other *Klebsormidium* and closely related *Interfilum* species (Karsten et al., 2010, 2014; Karsten and Holzinger, 2012). Low-light adaptation of photosynthesis in algae (indicated by high α and low I_c/I_k values) is usually coupled to more or less strong photoinhibition under enhanced photon fluence rates (Bischof et al., 1998 and references therein), and although our oxygen optode measurements were recorded only up to 500 μmol photons m^{-2} s^{-1}, the additionally measured rapid light curves (rETR) with a PAM 2500 up to 1432 μmol photons m^{-2} s^{-1} did also not indicate any photoinhibition. The conspicuously low light requirement is surprising for the African strains as South Africa is known for high insolation. A very nice explanation for low light adaptation under high solar radiation conditions is provided by Gray et al. (2007). These authors investigated BSCs of North American deserts where the abundant green microalgae vertically occupied microenvironments within the soil crust, which contributes to massive self-shading and hence protection from the damaging in-situ light field. The resulting differential susceptibility to enhanced photon fluence rates expressed by individual taxa indicates a complex spatial arrangement of the algal species in such a microhabitat, which seems to be structured in response to the vertical attenuation of irradiance (Gray et al., 2007). Under natural conditions, *Klebsormidium* species often form multi-layered structures interwoven with the upper millimetres of soil particles and other microorganisms, which most probably contribute to a high degree of self-shading and hence

photoprotection of individual filaments inside such an assemblage (Karsten et al., 2010). In contrast to the three African isolates from BSCs, precise habitat information on the Arctic Strain is missing. This species was isolated from snow in Northern Alaska, which is characterized as cold-desert region. But whether it occurred as crust-like assemblage or biofilm in or on top of snow is not reported. Port Barrow (Alaska) is located at 71°N and hence the annual surface incident solar radiation is about 40% less compared to the equator in combination with diurnal weather as well as seasonal changes between polar day and night (Thomas et al., 2008). Consequently, the Arctic Strain likely receives much lower insolation compared to the African strains. The four investigated *Klebsormidium* isolates exhibited all a high photophysiological plasticity which is in agreement with other investigated *Klebsormidium* species (Karsten et al., 2010; Karsten and Holzinger, 2012), pointing to genus-specific traits but also corresponding to findings in streptophyte green algae obtained from hydro-terrestrial habitats (Kaplan et al., 2013; Herburger et al., 2015). Since *Klebsormidium*, as member of the Streptophyta is considered as closely related to land plants, a set of potential protective mechanisms can be considered that have been developed by algae and embryophytes to counteract photoinhibition. These mechanisms limit the extent of photodamage (Raven, 2011), and include, for example, partial avoidance by restricting the number of photons incident on the photosynthetic apparatus by chloroplast movement. Other avoiding processes typically aim to dissipate excitation of photosynthetic pigments, for example, by non-photochemical quenching (e.g. xanthophyll cycle) or photochemical quenching (e.g. alternative electron transport pathways) (Raven, 2011). A recent publication on the *K. flaccidum* (superclade E) genome clearly indicates the presence of a basic system involved in high-light protection, which is considered as fundamental mechanism for algal adaptation to terrestrial habitats (Hori et al., 2014). This system includes cyclic electron flow activity at photosystem I, which is activated under radiation stress and desiccation (Hori et al., 2014). The cyclic electron flow is assumed to increase the proton gradient across the thylakoid membrane, which induces non-photochemical quenching and ATP biosynthesis, followed by the dissipation of excess radiation energy (Hori et al., 2014).

4.3. Temperature requirements of photosynthesis

Increasing temperatures had a strong effect on respiratory oxygen consumption and photosynthetic oxygen production in the four *Klebsormidium* strains and revealed isolate-specific differences (Fig. 4). While the cold-desert Arctic Strain showed optimal photosynthesis already at 15 °C (followed by a broad tolerance range), the three hot-desert African Strains exhibited maximum photosynthetic rates between 30 and 35 °C. At 40 °C only African Strain B had positive oxygen production rates, while in all other isolates photosynthesis was completely inhibited. These data indicate for the first time, that the temperature conditions of the natural habitat are reflected in the ecophysiological response patterns of the studied *Klebsormidium* strains, pointing to specific adaptations (genotypes) as discussed for acidophilic populations of *Klebsormidium* (Škaloud et al., 2014). Another aspect is the conspicuously different temperature requirement of photosynthesis and respiration. While respiratory rates were not detectable or very low at 5 and 10 °C in all studied strains, highest rates occurred between 30 and 45 °C, i.e. respiration under higher temperatures is more efficiently functioning than photosynthesis, while the opposite is true for lower temperatures, where photosynthesis typically exhibits enhanced activity rates

compared to respiration. This is also reflected in the P:R ratios (Fig. 5), which confirm a positive net carbon gain and hence biomass formation over a broad range between temperate (5 °C) and hot conditions (35–40 °C) in the African Strains, while the cold-desert Arctic Strain exhibited positive P:R values only under temperate conditions between 5 and 25 °C. These different tolerance widths reflect the natural hot and cold desert habitats, respectively. The disproportionate effect of temperature on photosynthesis and respiration in terrestrial green algae has also been documented in the closely related *K. crenulatum* and *K. dissectum*, both from alpine BSCs (Karsten et al., 2010; Karsten and Holzinger, 2012), and four different *Interfilum* strains from soil habitats (Karsten et al., 2014), as well as in *Prasiola crispa* from Antarctica (Davey, 1989). *Prasiola crispa* is a macroalgal member of the Trebouxiophyceae (Chlorophyta), and hence from an evolutionary view far distant from *Klebsormidium*. Nevertheless, similar physiological response patterns with rising temperatures strongly support the assumption that terrestrial green algae in general, and independent of their phylogenetic position, exhibit this trait. While photosynthesis is primarily controlled by light-related processes such as, for example, light absorption and energy transfer, respiration is typically influenced by temperature (Atkin and Tjoelker, 2003). Respiration of plants and algae is a complex process consisting of various enzymes, which exhibit different temperature optima and that are localized in different cellular compartments. The most sensitive respiratory enzyme would always act as a bottleneck affecting the whole process (Atkin and Tjoelker, 2003). The latter authors discussed the underlying acclimation mechanisms which include, for example, temperature-dependent changes in substrate availability, the maintenance of homeostatic levels of ATP synthesis across temperature gradients and/or reduction in the production of reactive oxygen species which are harmful for all metabolic functions.

4.4. Dehydration and rehydration

The desiccation experiments were undertaken by using a fully standardized approach (Karsten et al., 2014) to guarantee direct comparison between the 4 strains studied. While African Strain B exhibited a continuous decrease in the effective quantum yield from the beginning on over a period of 350 min down to zero signal, the other 3 samples showed an unchanged maximum ΔF/Fm′ for some time before a threshold was reached after which the fluorescence signals strongly decreased (Fig. 7). The interval of unaffected ΔF/Fm′ was much longer in African Strains A and C, compared to the Arctic Strain. These differences in the ΔF/Fm′ kinetics during desiccation can be explained by the isolate-specific morphologies. African Strains A and C are characterized by long uniserate filaments and much thicker, mechanically more stable cells compared to the single small cells or short cell filaments of African Strain B and the Arctic Strain, respectively (Fig. 1). Similar response patterns had been recently reported for various isolates of the closely related *Interfilum* (Karsten et al., 2014), which exhibited also striking differences in morphology. Single-cell strains of *Interfilum* were much more sensitive to desiccation than algal cells inhabiting an aggregate, colony or biofilm, all representing morphological structures which hamper or at least retard water loss.

Recovery kinetics of ΔF/Fm′ after rehydration of the dried *Klebsormidium* samples also exhibited conspicuous strain-specific differences. Except African Strain A, all other isolates

fully recovered upon rehydration with fluid water. African Strain A showed only 20% of the control effective quantum yield, which points to some damage in the photosynthetic apparatus. The recovery kinetics of the African Strains B and C and the Arctic Strain were similar to those of *Interfilum* (Karsten et al., 2014) and an aeroterrestrial green algal biofilm occurring on top of a building façade (Häubner et al., 2006). This biofilm also showed a quick recovery of ΔF/Fm′ after artificial moistening (Häubner et al., 2006). Such high dehydration tolerance in conjunction with high recovery rates seems to be a typical feature of many terrestrial green algae from alpine, dune and dryland BSCs (De Winder et al., 1990; Gray et al., 2007; Karsten et al., 2010; Karsten and Holzinger, 2012; Holzinger and Karsten, 2013). The underlying mechanisms have been recently touched for the first time in *Klebsormidium crenulatum* using a transcriptomic approach (Holzinger et al., 2014). These authors reported also a strong inhibition of ΔF/Fm′ during desiccation, but, for example, in parallel the up-regulation of transcripts for photosynthesis, energy production, reactive oxygen species metabolism, as well as of plant proteins involved in early response to desiccation (ERD) or enzymes for oligosaccharide biosynthesis. The most important conclusion was the first experimental proof that streptophyte green algae exhibit similar molecular events during desiccation stress than land plants pointing to ancestral mechanisms for the successful colonization of terrestrial habitats (Holzinger et al., 2014). Future studies should take the strain and clade specific differences shown here into account, and our biological understanding of the underlying mechanisms will largely benefit when not only investigating one selected model organism.

Acknowledgements

The present study was undertaken during the first author’s sabbatical at the University of Innsbruck, and it was supported by a grant from the Deutsche Forschungsgemeinschaft (DFG) (KA899/16-1/2/3/4) (U.K.), as well as a FWF grant P24242-B16 and FWF grant I 1951-B16 (A.H.). Our sincere thanks are extended to Prof. Burkhard Büdel (University of Kaiserslautern) for providing the BIOTA strains, as well as to Dr. Tatiana Mikhailyuk (M.H. Kholodny Institute of Botany, National Academy of Sciences of Ukraine) for information concerning the phylogenetic positions of the isolates used.

References

Atkin OK, Tjoelker MG. Thermal acclimation and the dynamic response of plant respiration to temperature. Trends Plant Sci. 2003; 8:343–351. [PubMed: 12878019]

Belnap, J.; Lange, OL. Biological Soil Crusts: Structure, Function and Management. Springer; Berlin: 2001.

Bischof K, Hanelt D, Tüg H, Karsten U, Brouwer PEM, Wiencke C. Acclimation of brown algal photosynthesis to ultraviolet radiation in Arctic coastal waters (Spitsbergen, Norway). Polar Biol. 1998; 20:388–395.

Büdel B, Darienko T, Deutschewitz K, Dojani S, Friedl T, Mohr KI, et al. Southern African biological soil crusts are ubiquitous and highly diverse in drylands, being restricted by rainfall frequency. Microb. Ecol. 2009; 57:229–247. [PubMed: 18850242]

Castillo-Monroy AP, Maestre FT, Delgado-Baquerizo M, Gallardo A. Biological soil crust modulate nitrogen availability in semi-arid ecosystem: insights from a Mediterranean grassland. Plant Soil. 2010; 333:21–34.

Davey MC. The effects of freezing and desiccation on photosynthesis and survival of terrestrial Antarctic algae and cyanobacteria. Pol. Biol. 1989; 10:29–36.

De Winder B, Matthijs HCP, Mur LR. The effect of dehydration and ion stress on carbon dioxide fixation in drought-tolerant phototrophic micro-organisms. FEMS Microbiol. Ecol. 1990; 74:33–38.

Elbert W, Weber B, Burrows S, Steinkamp J, Büdel B, Andreae MO, Pöschl U. Contribution of crytogamic covers to the global cycles of carbon and nitrogen. Nat. Geosci. 2012; 5:459–462.

Genty B, Briantais JM, Baker NR. The relationship between the quantum yield of photosynthetic electron-transport and quenching of chlorophyll fluorescence. Biochim Biophys. Acta. 1989; 990:87–92.

Gray DW, Lewis LA, Cardon ZG. Photosynthetic recovery following desiccation of desert green algae (Chlorophyta) and their aquatic relatives. Plant Cell Environ. 2007; 30:1240–1255. [PubMed: 17727415]

Häubner N, Schumann R, Karsten U. Aeroterrestrial algae growing on facades—response to temperature and water stress. Microb. Ecol. 2006; 51:285–293. [PubMed: 16596441]

Herburger K, Lewis LA, Holzinger A. Photosynthetic efficiency, desiccation tolerance and ultrastructure in two phylogenetically distinct strains of alpine *Zygnema* sp. (Zygnematophyceae, Streptophyta): role of pre-akinete formation. Protoplasma. 2015; 252:571–589. [PubMed: 25269628]

Holzinger A, Lütz C, Karsten U. Desiccation stress causes structural and ultra-structural alterations in the aeroterrestrial green alga *Klebsormidium crenulatum* (Klebsormidiophyceae, Streptophyta) isolated from an alpine soil crust. J. Phycol. 2011; 47:591–602. [PubMed: 27021989]

Holzinger A, Karsten U. Desiccation stress and tolerance in green algae: consequences for ultrastructure, physiological and molecular mechanisms. Front. Plant Sci. 2013; 4 article 327.

Holzinger A, Kaplan F, Blaas K, Zechmann B, Komsic-Buchmann K, Becker B. Transcriptomics of desiccation tolerance in the streptophyte green alga *Klebsormidium* reveal a land plant-like defense reaction. PLoS One. 2014; 9:e110630. [PubMed: 25340847]

Hori K, Maruyama F, Fujisawa T, Togashi T, Yamamoto N, Seo M, et al. Klebsormidium flaccidum genome reveals primary factors for plant terrestrial adaptation. Nat. Commun. 2014; 5 http://dx.doi.org/10.1038/ncomms4978.

Kaplan F, Lewis LA, Wastian J, Holzinger A. Plasmolysis effects and osmotic potential of two phylogenetically distinct alpine strains of *Klebsormidium* (Streptophyta). Protoplasma. 2012; 249:789–804. [PubMed: 21979310]

Kaplan F, Lewis LA, Herburger K, Holzinger A. Osmotic stress in the Arctic and Antarctic green alga *Zygnema* sp. (Zygnemtales, Streptophyta): effects on photosynthesis and ultrastructure. Micron. 2013; 44:317–330. [PubMed: 22959821]

Karsten U, Lütz C, Holzinger A. Ecophysiological performance of the aeroterrestrial green alga *Klebsormidium crenulatum* (Klebsormidiophyceae, Streptophyta) isolated from an alpine soil crust with an emphasis on desiccation stress. J. Phycol. 2010; 46:1187–1197.

Karsten U, Holzinger A. Light, temperature and desiccation effects on photosynthetic activity, and drought-induced ultrastructural changes in the green alga *Klebsormidium* disectum (Streptophyta) from a high alpine soil crust. Microb. Ecol. 2012; 63:51–63. [PubMed: 21811791]

Karsten U, Holzinger A. Green algae in alpine biological soil crust communities: acclimation strategies against ultraviolet radiation and dehydration. Biodivers. Conserv. 2014; 23:1845–1858. [PubMed: 24954980]

Karsten U, Herburger K, Holzinger A. Dehydration, temperature and light tolerance in members of the aeroterrestrial green algal genus Interfilum (Streptophyta) from biogeographically different temperate soils. J. Phycol. 2014; 50:804–816. [PubMed: 25810561]

Kitzing C, Pröschold T, Karsten U. UV-induced effects on growth, photosynthetic performance and sunscreen contents in different populations of the green alga *Klebsormidium fluitans* (Streptophyta) from alpine soil crusts. Microb. Ecol. 2014; 67:327–340. [PubMed: 24233286]

Kitzing C, Karsten U. UV-induced effects on optimum quantum yield and sunscreen contents in members of the genera Interfilum, *Klebsormidium*, Hormidiella and Entransia (Klebsormidiophyceae, Streptophyta). Eur. J. Phycol. 2015; 50:279–287.

Kromkamp JC, Forster RM. The use of variable fluorescence measurements in aquatic ecosystems: differences between multiple and single turnover measuring protocols and suggested terminology. Eur. J. Phycol. 2003; 38:103–112.

Mikhailyuk T, Holzinger A, Massalski A, Karsten U. Morphological and ultrastructural aspects of Interfilum and *Klebsormidium* (Klebsormidiales, Streptophyta) with special reference to cell division and thallus formation. Eur. J. Phycol. 2014; 49:395–412. [PubMed: 26504365]

Mikhailyuk TI, Sluiman HJ, Massalski A, Mudimu O, Demchenko EM, Kondratyuk SY, Friedl T. New streptophyte green algae from terrestrial habitats and an assessment of the genus Interfilum (Klebsormidiophyceae, Streptophyta). J. Phycol. 2008; 44:1586–1603. [PubMed: 27039871]

Porra RJ, Thompson WA, Kriedmann PE. Determination of accurate extinction coefficients and simultaneous equations for assaying chlorophylls a and b extracted with four different solvents: verification of the concentration of chlorophyll standards by atomic absorption spectroscopy. BBA–Bioenerg. 1989; 975:384–394.

Raven JA. The cost of photoinhibition. Physiol. Plant. 2011; 142:87–104. [PubMed: 21382037]

Remias D, Albert A, Lütz C. Effects of simulated, but realistic, elevated UV irradiation on photosynthesis and pigment composition of the alpine snow alga Chlamydomonas nivalis and the Arctic soil alga *Tetracystis* sp. (Chlorophyceae). Photosynthetica. 2010; 48:269–277.

Rindi F, Mikhailyuk TI, Sluiman HJ, Friedl T, Lopez-Bautista JM. Phylogenetic relationships in Interfilum and *Klebsormidium* (Klebsormidiophyceae, Streptophyta). Mol. Phylogenet. Evol. 2011; 58:218–231. [PubMed: 21145975]

Ryšánek D, Hrčková K, Škaloud P. Global ubiquity and local endemism of free-living terrestrial protists: phylogeographic assessment of the streptophyte alga *Klebsormidium*. Environ. Microbiol. 2015; 17:689–698. [PubMed: 24803402]

Schreiber U, Bilger W. Progress in chlorophyll fluorescence research: major developments during the past years in retrospect. Prog. Bot. 1993; 54:151–173.

Škaloud P, Lukešová A, Malavasi V, Ryšánek D, Hrčková K, Rindi F. Molecular evidence for the polyphyletic origin of low pH adaptation in the genus *Klebsormidium* (Klebsormidiophyceae, Streptophyta). Plant Ecol. Evol. 2014; 147:333–345.

Silva PC, Mattox KR, Blackwell WH. The generic name Hormidium as applied to green algae. Taxon. 1972; 21:639–645.

Starr RC, Zeikus JA. UTEX—the culture collection of algae at the University of Texas at Austin 1993 list of cultures. J. Phycol. 1993; 29:1–106.

Thomas, DN.; Fogg, GE.; Convey, P.; Fritsen, CH.; Gili, JM.; Gradinger, R.; Laybourn-Parry, J.; Reid, K.; Walton, DWH. The Biology of Polar Regions. Oxford University Press; Oxford: 2008.

Ullmann, I.; Büdel, B. Biological soil crusts of Africa. Springer; Berlin: 2001. p. 107-108. Ecological Studies 150

Webb WL, Newton M, Starr D. Carbon dioxide exchange of Alnus rubra: a mathematical model. Oecologia. 1974; 17:281–291.

Yoshitake S, Uchida M, Koizumi H, Kanda H, Nakatsubo T. Production of biological soil crusts in the early stage of primary succession on a High Arctic glacier foreland. New Phytol. 2010; 186:451–460. [PubMed: 20136719]

Europe PMC Funders Author Manuscripts

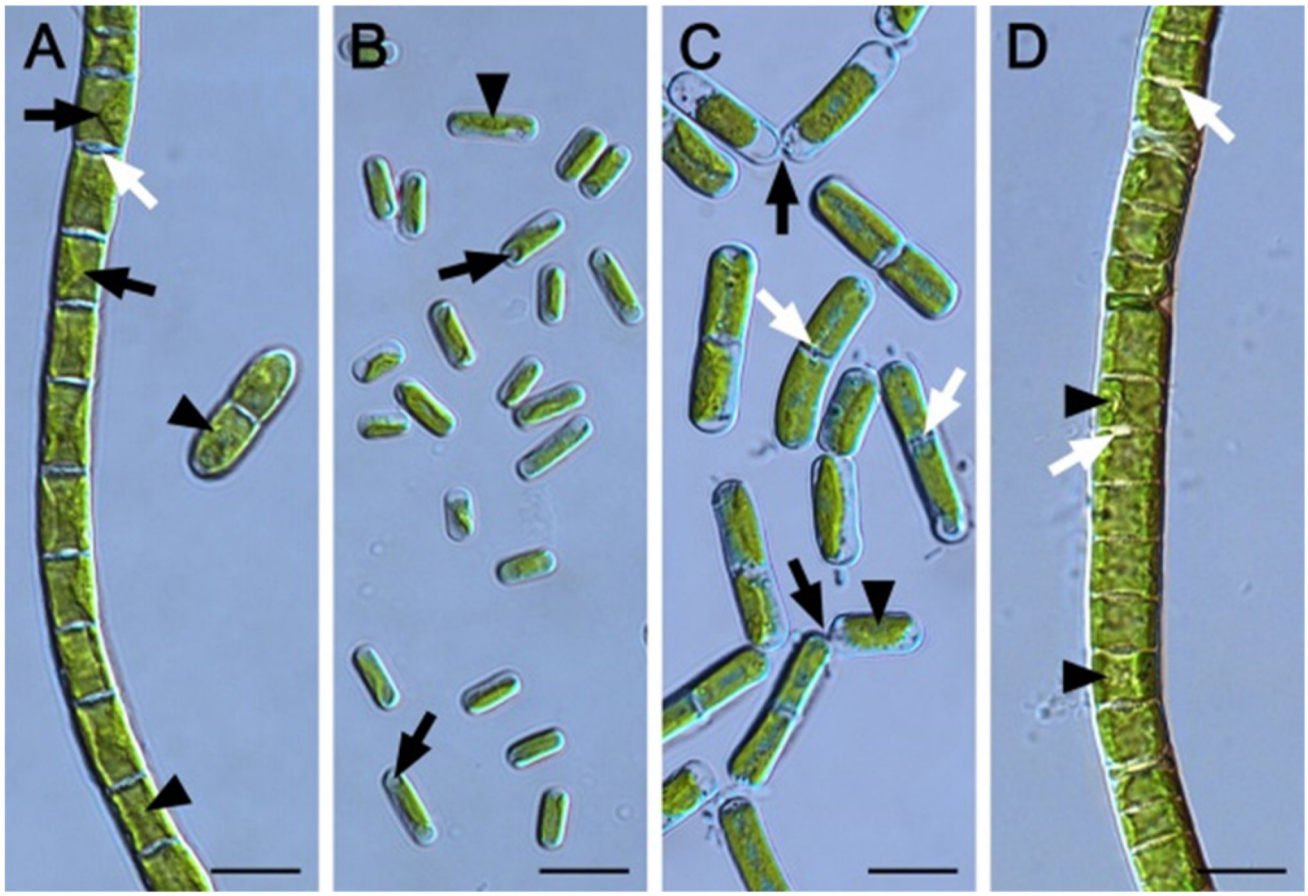

Fig. 1.

Morphology of the four *Klebsormidium* strains (Klebsormidiales, Streptophyta) BIOTA 14614.7 (African Strain A) (A), BIOTA 14613.5e (African Strain B) (B), SAG 384-1 (Arctic Strain) (C) and BIOTA 14614.18.24 (African Strain C) (D) taken from 1 month old liquid cultures. (A) Cell filament and 2-cell-fragment with clearly visible pyrenoids (arrowheads), cross-wall protuberances (white arrow) and parietal chloroplasts with margins protruding towards the cell centre (black arrows). (B) Ovoid and cylindrical individual cells with one pyrenoid per cell (arrowhead) and spherical chloroplast-free districts at the cell poles (arrows). (C) Short cell filaments and detaching cells (black arrows). Pyrenoids are marked with arrowheads and cross-wall protuberances with white arrows. (D) Cell filament with pyrenoids (arrowheads) and prominent cross-wall protuberances (arrows). Scale bars equal always 10 μm.

Europe PMC Funders Author Manuscripts

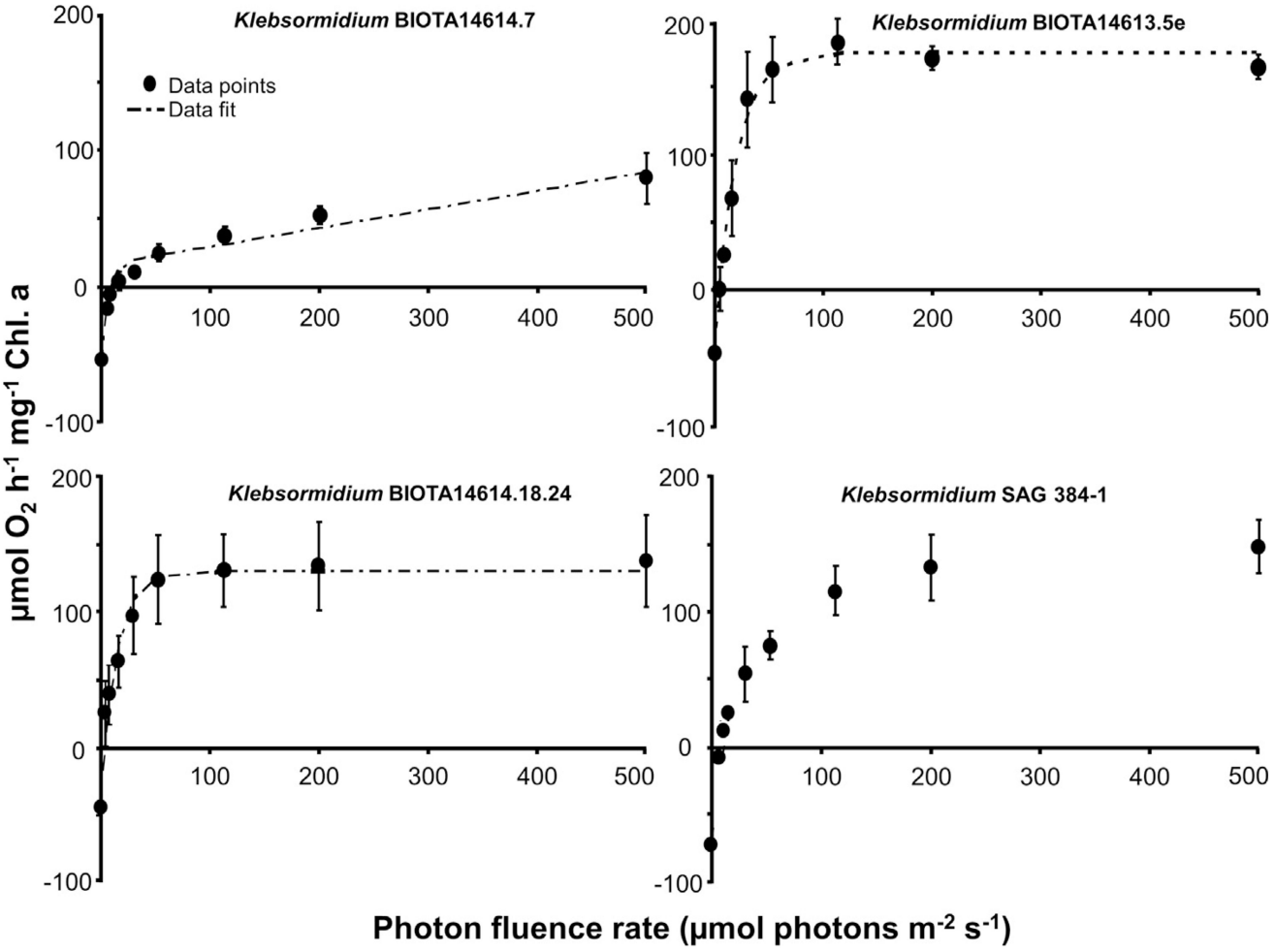

Fig. 2.

Dark respiration and photosynthetic oxygen evolution as function of increasing photon fluence densities up to 500 µmol photons m^{-2} s^{-1} in the four *Klebsormidium* isolates BIOTA 14614.7 (African Strain A), BIOTA 14613.5e (African Strain B), BIOTA 14614.18.24 (African Strain C) and SAG 384-1 (Arctic Strain) (n = 3, mean value ± SD). The dotted line represents in the 3 African Strains a fitted curve of the data measured according the photosynthesis model of Webb et al. (1974).

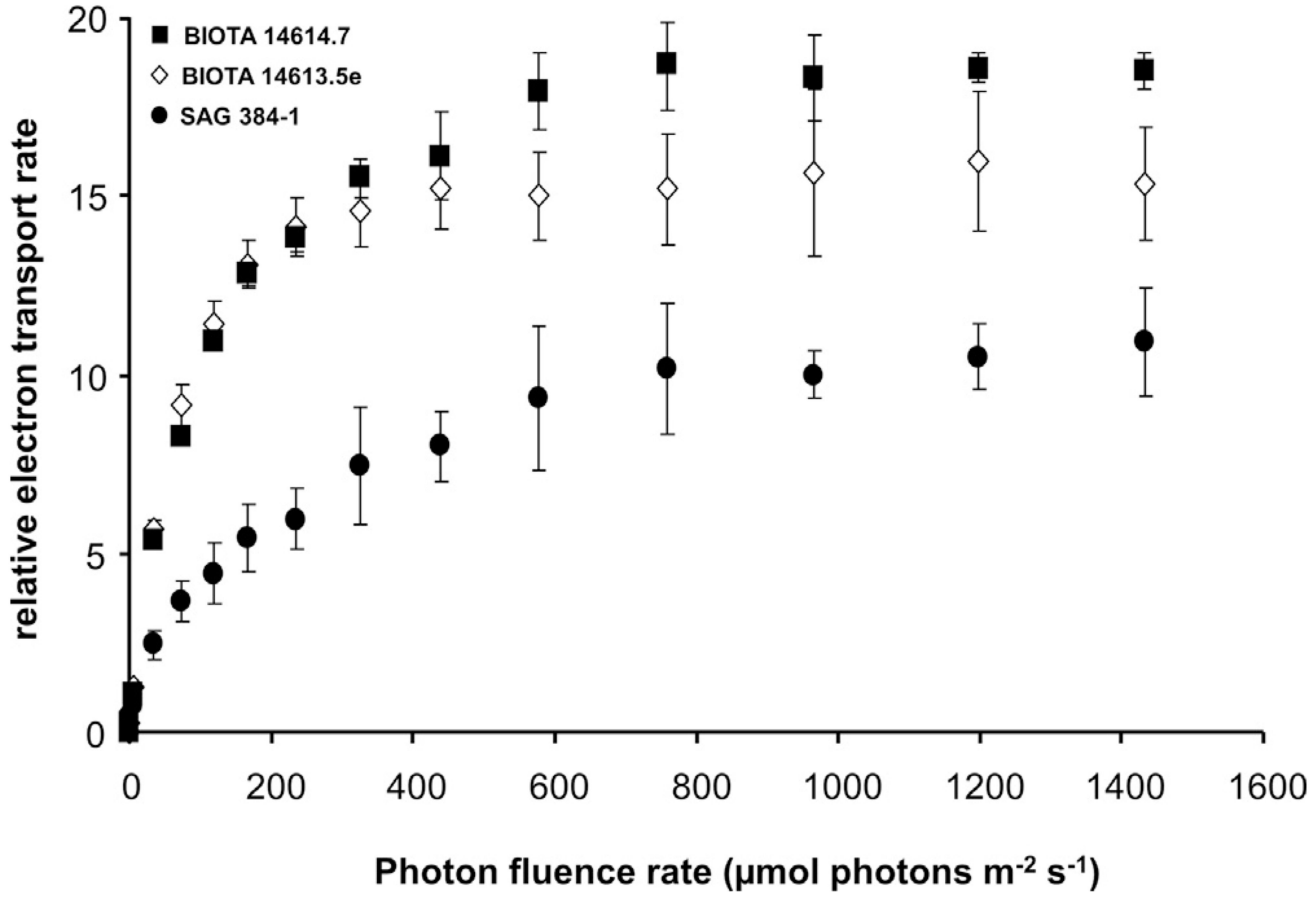

Fig. 3.

The effect of increasing photon fluence densities up to 1432 µmol photons m^{-2} s^{-1} on the relative electron transport rate (rETR, µmol electrons m^{-2} s^{-1}) in 3 of the studied *Klebsormidium* strains (n = 4, mean value ± SD). BIOTA 14614.7 (African Strain A), BIOTA 14613.5e (African Strain B), and SAG 384-1 (Arctic Strain). BIOTA 14614.18.24 (African Strain C) showed the same curve shape as BIOTA 14613.5e (African Strain B) and hence was not shown. All measurements were done at 22 ± 1 °C.

Europe PMC Funders Author Manuscripts

Europe PMC Funders Author Manuscripts

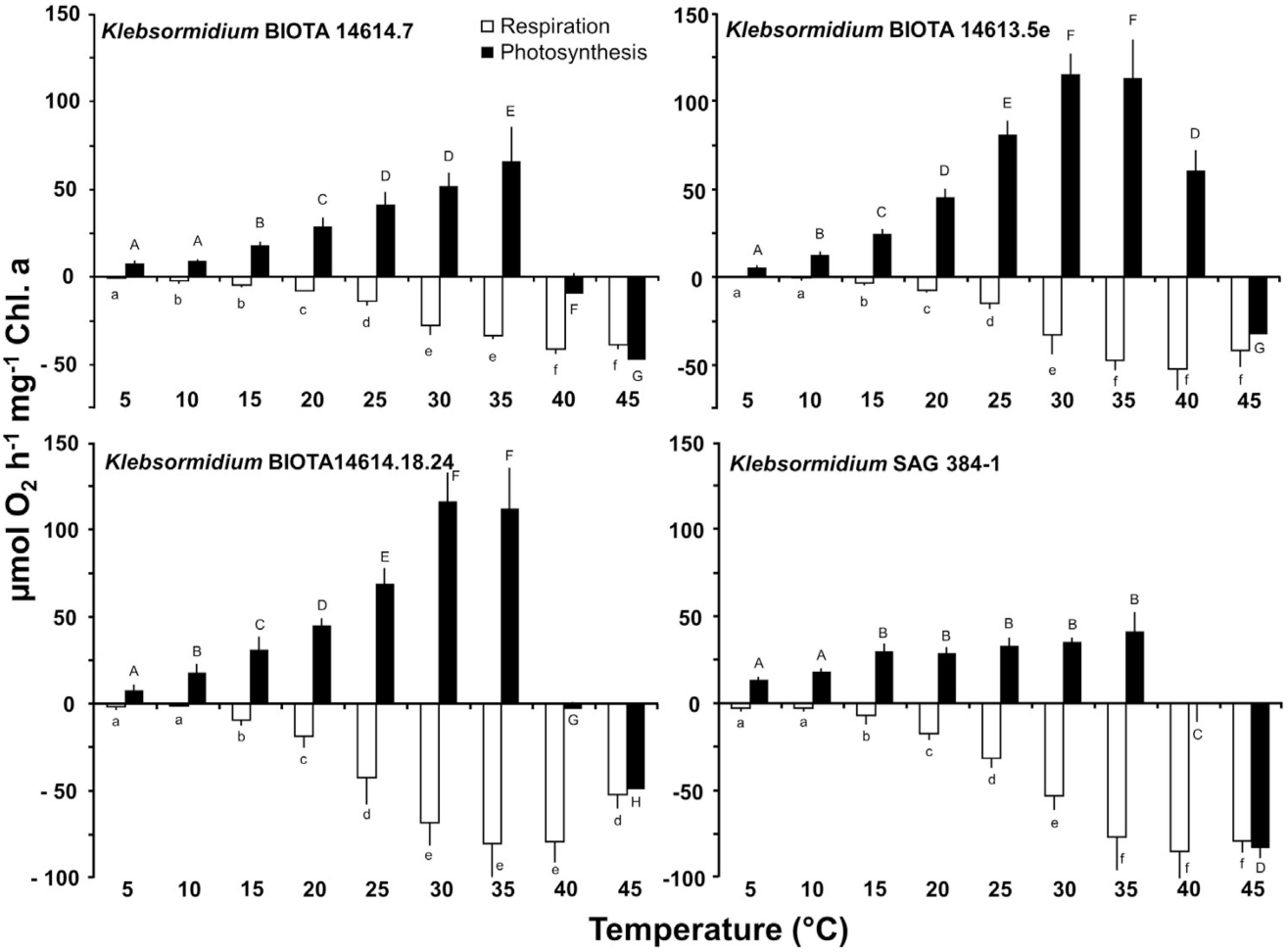

Fig. 4.

Photosynthetic oxygen development and respiratory oxygen consumption in µmol O_2 h^{-1} mg^{-1} Chl. a measured at 200 µmol photons m^{-2} s^{-1} as function of increasing temperatures in the four studied strains of *Klebsormidium* (n = 3, mean value ± SD), BIOTA 14614.7 (African Strain A), BIOTA 14,613.5e (African Strain B), BIOTA 14,614.18.24 (African Strain C) and SAG 384-1 (Arctic Strain). Significances among the treatments were calculated by one-way ANOVA ($p < 0.001$). Different capital (net photosynthesis) and small letters (respiration) represent significant differences among the temperatures as revealed by Tukey's post hoc test.

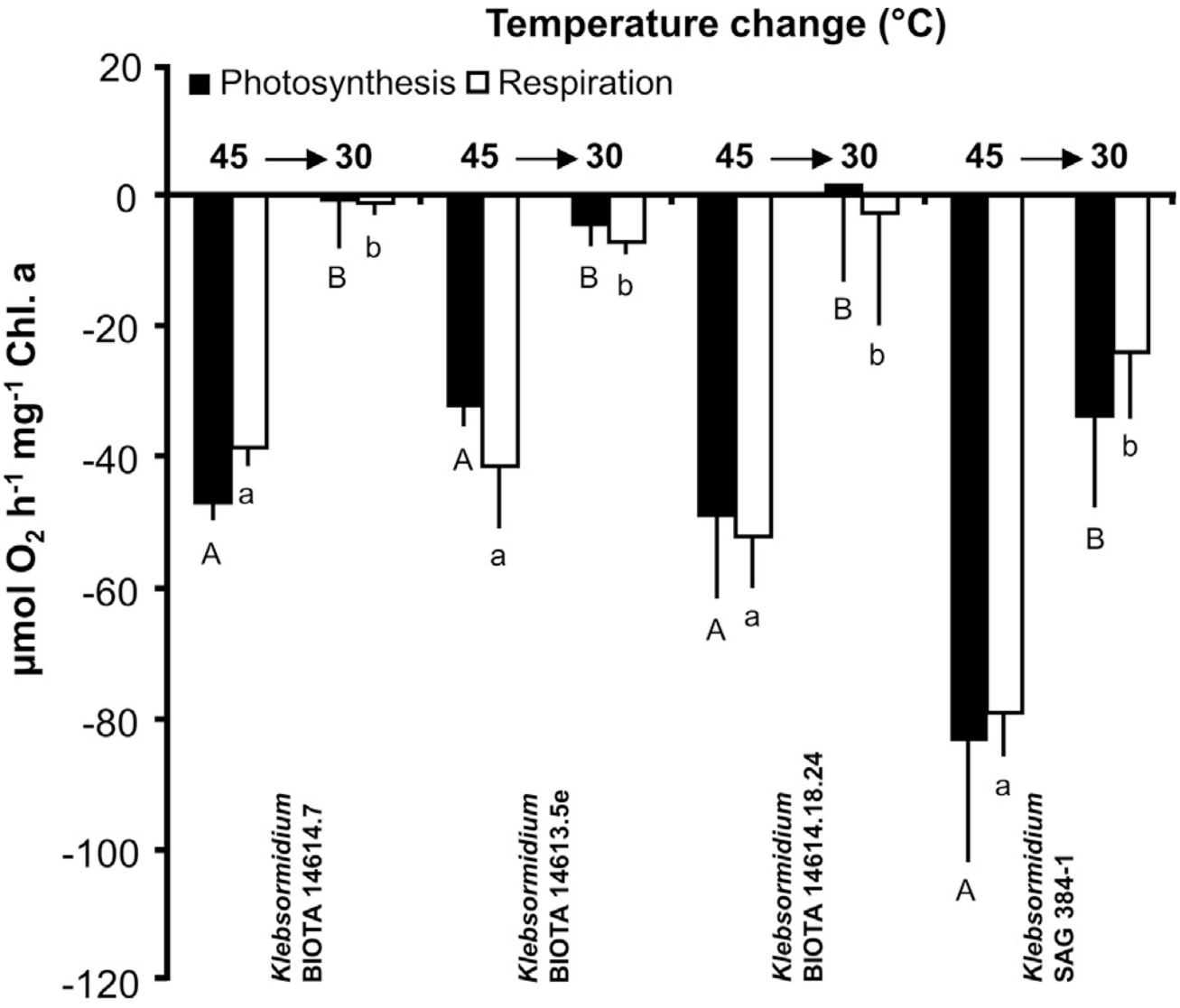

Fig. 5.

Photosynthesis and respiration in µmol O_2 h^{-1} mg^{-1} Chl. a measured at 200 µmol photons m^{-2} s^{-1} at 45 °C (see Fig. 3) and after transfer back to 30 °C in the four studied strains of *Klebsormidium* (n = 3, mean value ± SD), BIOTA 14614.7 (African Strain A), BIOTA 14,613.5e (African Strain B), BIOTA 14614.18.24 (African Strain C) and SAG 384-1 (Arctic Strain). Significances among the treatments were calculated by one-way ANOVA (p < 0.001). Different capital (photosynthesis) and small letters (respiration) represent significant differences among the temperatures as revealed by Tukey's post hoc test.

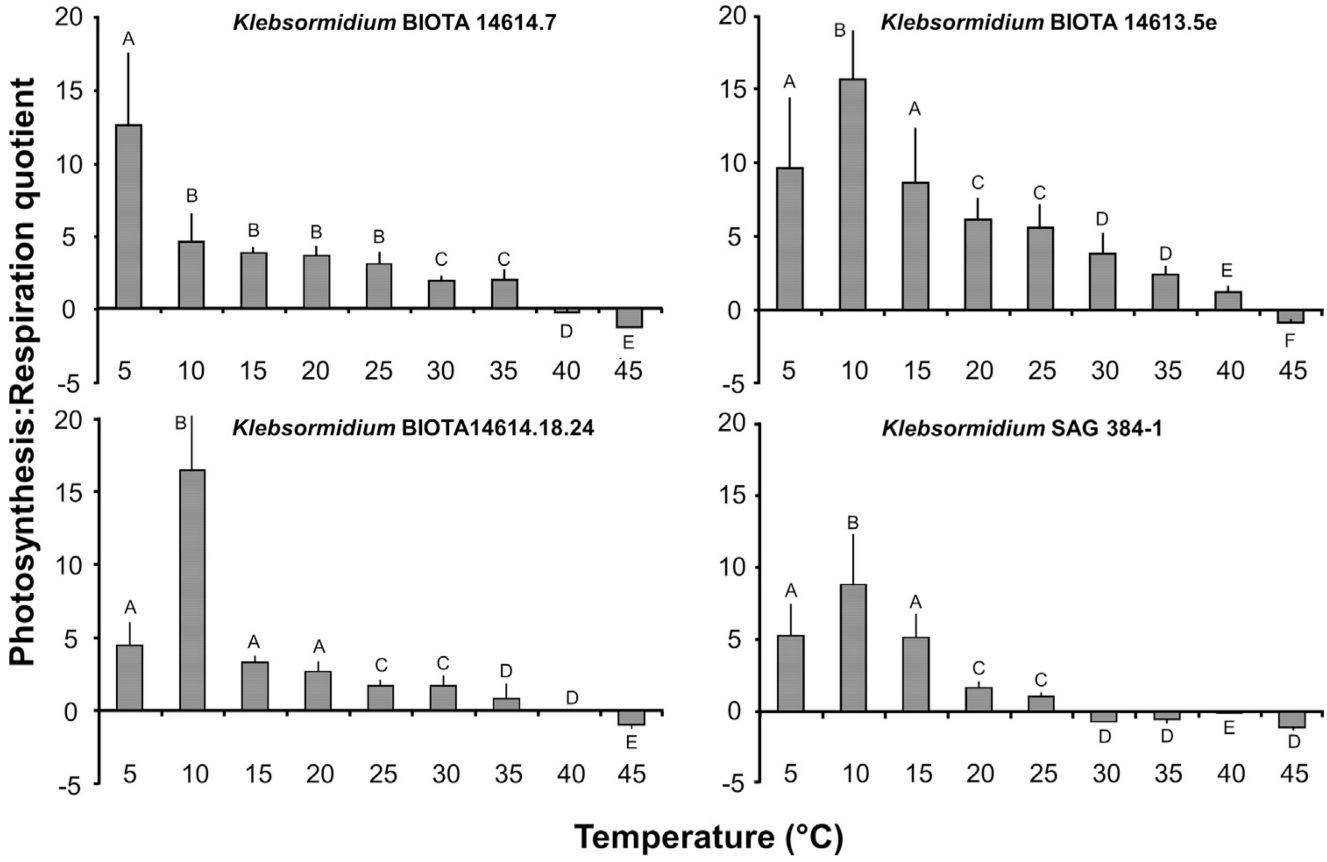

Fig. 6.

Photosynthesis:respiration (P:R) quotient as function of increasing temperatures in the four *Klebsormidium* isolates BIOTA 14,614.7 (African Strain A), BIOTA 14613.5e (African Strain B), BIOTA 14614.18.24 (African Strain C) and SAG 384-1 (Arctic Strain) ($n = 3$, mean value ± SD). Significances among the treatments were calculated by one-way ANOVA ($p < 0.001$). Different capital letters represent significant differences among the temperatures as revealed by Tukey's post hoc test.

Europe PMC Funders Author Manuscripts

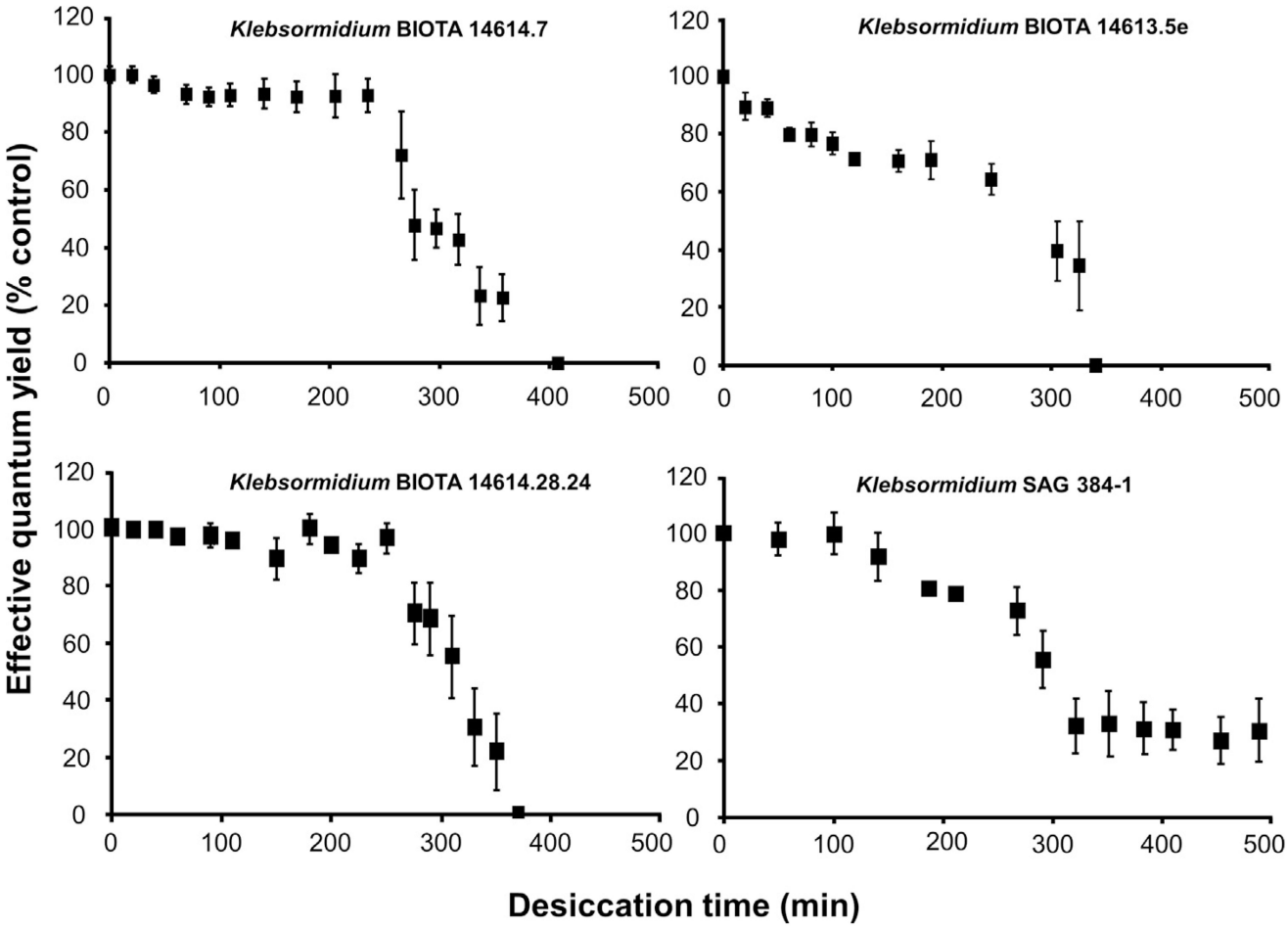

Fig. 7.

The effect of controlled desiccation on the effective quantum yield (ΔF/Fm′) of photosystem 2 as regularly measured with a PAM 2500 during the experiment (400–500 min) in the four *Klebsormidium* isolates BIOTA 14614.7 (African Strain A), BIOTA 14,613.5e (African Strain B), BIOTA 14614.18.24 (African Strain C) and SAG 384-1 (Arctic Strain) ($n = 4$, mean value±SD). Effective quantum yield values of control algae under 40 µmol photons m^{-2} s^{-1} PAR was determined as 0.54–0.59 and standardized to 100% for better comparison. All measurements were done at 22 ± 1 °C.

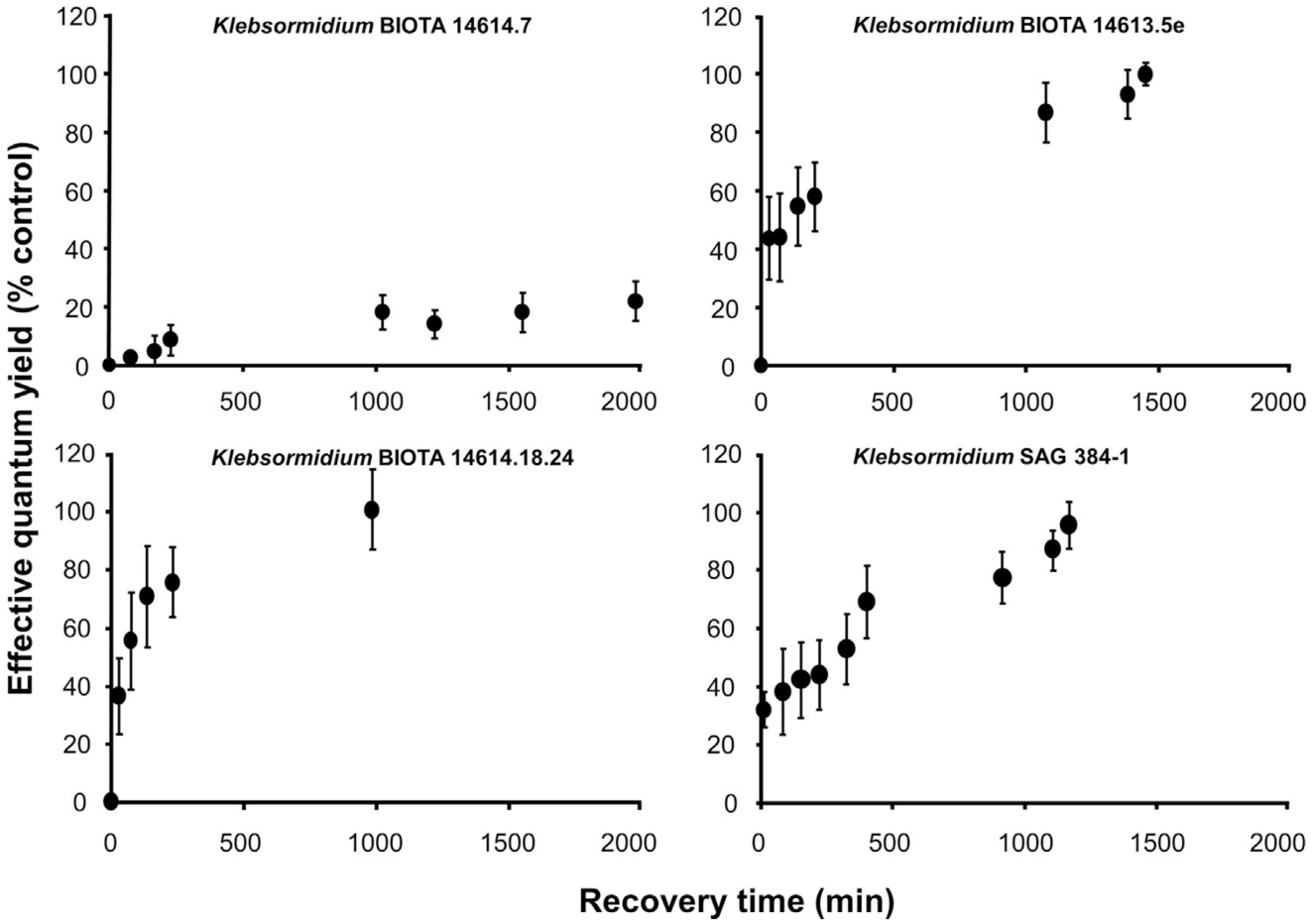

Fig. 8.

The effect of controlled rehydration on the effective quantum yield (ΔF/Fm′) of photosystem 2 in the desiccated algal samples (see Fig. 6) as measured with a PAM 2500 during the experiment (1000–2000 min depending on the response) in the four *Klebsormidium* isolates BIOTA 14614.7 (African Strain A), BIOTA 14613.5e (African Strain B), BIOTA 14614.18.24 (African Strain C) and SAG 384-1 (Arctic Strain) ($n = 4$, mean value ± SD). Effective quantum yield values of control algae under 40 µmol photons m^{-2} s^{-1} PAR was determined as 0.54–0.59 and standardized to 100% for better comparison. All measurements were done at 22 ± 1 °C.

Europe PMC Funders Author Manuscripts

Table 1

Characterization of the *Klebsormidium* isolates collected from dry regions. Strain number, habitat and origin, taxonomic assignment according to the suggested clades of Rindi et al. (2011) are given. The meteorological data include monthly air temperature, monthly rainfall days, monthly precipitation (mm) and annual precipitation (mm) (www.worldweatheronline.com). The sequence accession numbers include complete and partial sequences, respectively, of the different ribosomal regions. SAG: Sammlung für Algenkulturen, Göttingen, Germany.

Assigned species, strain number and synonym used in the text	Habitat and origin	Meteorological data	Clade assignment according to Rindi et al. (2011)	Sequence Accession (18s rRNA, ITS1, 5.8s rRNA, ITS2, 28s rRNA)
Klebsormidium sp. BIOTA 14614.7 African Strain A	Biological soil crust, BIOTA observatory Grootderm, succulent Karoo, South Africa 28°36′44.1″ S 16°39′45.0″ E leg.: Burkhard Büdel 14 March 2001	Air temperature: 13.5–20.6 °C Monthly rainfall days: 0–14 Monthly precipitation: 0 to 34.2 mm Annual rainfall: 56 mm	G	HF955429.1
Klebsormidium sp. BIOTA 14613.5e African Strain B	Biological soil crust, BIOTA observatory Koeboes, South Africa, 28°45′51.1″S 16°98′38.3″ E leg.: Burkhard Büdel 12 March 2001	As above	G	HF955431.1
Klebsormidium sp. BIOTA 14614.18.24 African Strain C	Biological soil crust, BIOTA observatory Grootderm, succulent Karoo, South Africa, 28°36′44.5″ S 16°39′52.4″ E leg.: Burkhard Büdel 14 March 2001	As above	G	HF955428.1
Klebsormidium subtilissimum SAG 384-1 Arctic Strain	Snow, Port Barrow, Alaska, USA; cold-desert climate isolated 1952 R.A. Lewin	Air temperature: −29.1–8.3 °C Monthly rainfall days: 4 to 12 Monthly precipitation: 2.3–26.7 mm Annual rainfall: 114 mm	E6	EF372517.1

Europe PMC Funders Author Manuscripts

Table 2

Cell dimensions (length and width in µm) and length:width (L:W) ratio of the four *Klebsormidium* strains investigated ($n = 20 \pm SD$). Capital letters (length), small letters (width) and cursive small letters (L:W ratio) indicate significant differences between the dimensions. Data were analysed by one-way ANOVA followed by Tukey's post hoc test ($p < 0.001$). Cell length and width of each strain was compared by a standard two-sample *t* test and significantly differences are marked with an asterisk ($p < 0.001$).

	Length	Width	L:W ratio
BIOTA 14614.7	7.8 ± 1.2^{A}	$6.8 \pm 0.3^{a*}$	1.2 ± 0.2^{a}
BIOTA 14613.5e	7.6 ± 1.4^{A}	$4.1 \pm 0.4^{b*}$	1.9 ± 0.4^{b}
SAG 384-1	13.7 ± 4.0^{B}	$5.5 \pm 0.5^{c*}$	2.5 ± 0.8^{c}
BIOTA 14614.18.24	8.0 ± 2.1^{A}	8.8 ± 1.0^{d}	0.9 ± 0.3^{a}

Table 3

Photosynthesis-irradiance curve parameters of the *Klebsormidium* strains studied. Data were recorded as oxygen evolution using an oxygen optode at 25 °C and for the 3 African Strains fitted with the photosynthesis model of Webb et al. (1974) without photoinhibition. α: positive slope at limiting photon fluence rates (μmol O_2 mg^{-1} Chl. *a* (μmol photons m^{-2} s^{-1})$^{-1}$); I_c: light compensation point (μmol photons m^{-2} s^{-1}); I_k: initial value of light-saturated photosynthesis (μmol photons m^{-2} s^{-1}). In addition, the chlorophyll *a*: chlorophyll *b* ratios are given. Data represent mean values ± SD of 3 replicates. The significance of differences among the strains, as indicated by different letters (capital letters for α; small letters for I_c; cursive capital letters for I_k) was calculated by one-way ANOVA ($p < 0.001$) and Tukey's post hoc test.

Strain number	α	I_c	I_k	Chl. a: Chl. b
Klebsormidium sp. BIOTA 14614.7 (African Strain A)	5.73 ± 1.39^{A}	14.65 ± 2.27^{a}	18.83 ± 2.69^{A}	2.43 ± 0.26^{a}
Klebsormidium sp. BIOTA 14613.5e (African Strain B)	10.93 ± 2.56^{B}	4.44 ± 0.78^{b}	19.99 ± 3.16^{A}	2.10 ± 0.31^{a}
Klebsormidium sp.BIOTA 14614.18.24(African Strain C)	12.40 ± 1.96^{B}	5.86 ± 1.19^{b}	14.11 ± 2.71^{B}	2.07 ± 0.17^{a}
Klebsormidium subtilissimum SAG 384-1 (Arctic Strain)	8.29 ± 2.63^{B}	10.55 ± 2.09^{a}	23.56 ± 3.34^{A}	1.86 ± 0.15^{b}